

Lasers in Manufacturing Conference 2025

Investigations on the detectability of penetration depth fluctuations in laser welding by means of optical coherence tomography

Lucas Westermeyer^{a,b,*}, Annika Bohlen^a, Thomas Seefeld^{a,b}

^aBIAS—Bremer Institut für angewandte Strahltechnik GmbH, Klagenfurter Straße 5, Bremen 28359, Germany

^bMAPEX Center for Materials and Processes, Universität Bremen, Bibliothekstraße 1, Bremen 28359, Germany

Abstract

Optical coherence tomography (OCT) can be used to determine the depth of the keyhole during laser deep penetration welding. However, due to the nature of the OCT-data a statistical evaluation approach is necessary, reducing the possible temporal resolution. At the same time, keyhole welding is a strongly dynamic process, and the penetration depth of welds can fluctuate even under constant process parameters. In this study the limits of detecting weld depth fluctuations by common methods for filtering OCT-data are investigated. First the magnitudes of weld depth fluctuations are measured for the materials steel (DC-01), aluminum (EN AW-1050) and Copper (Cu-ETP) by examining longitudinal cross sections. Secondly common filtering methods are tested on simulated OCT-data in a controlled environment and evaluated in the context of the measurement frequency of the OCT-system. Results show that the weld depth fluctuations are severest in aluminum, followed by copper. The detection of the fastest fluctuations in aluminum using basic filter approaches may present difficulties mainly caused by declining filter accuracy when limited amounts of data are available. Higher OCT measurement frequencies help to solve this problem.

Keywords: keyhole welding; optical coherence tomography; process control

1. Introduction

Laser deep penetration welding is achieved by focusing a high-power laser onto a metallic surface, which causes it to be heated past its evaporation temperature. The resulting recoil pressure pushes the molten material downwards, creating a vapor capillary, often called a keyhole. A high absorption is achieved due to the laser being reflected multiple times at the walls of the keyhole, allowing for high weld depths. The keyhole itself is strongly dynamic even under constant process parameters as its shape and depth can change rapidly, which can be the cause of defects such as pores or weld depth fluctuations. Especially in overlap welds, where the desired weld depth is close to the total thickness of the joining partners, changes in the weld depth can lead to full penetration of the lower joining partner. These weld through defects can damage functional layers or aesthetic surfaces.

Different approaches for closed loop control of the weld depth for the prevention of weld through defects have already been implemented. These include indirect estimations of the weld depth using spectrometric measurements (Konuk et al. 2011) or camera based methods (Kos et al. 2021). One increasingly popular way to directly measure the weld depth is optical coherence tomography (OCT), which was demonstrated by (Bautze and Kogel-Hollacher, 2014). More specifically, a spectral domain OCT is an Interferometric distance measurement tool capable of measuring the keyhole depth by coaxially coupling a probe beam into the processing laser and thus into the keyhole. The reflected light from the keyhole bottom produces an interference with a reference beam, which is then measured with a spectrometer. A depth spectrum is calculated by the Fourier transform of the interference pattern, in which surfaces at which the probe beam was reflected show up as peaks. (Fercher et al. 2003). Peaks in the depth spectrum are then detected as datapoints containing a depth information in their location on the depth spectrum as well as a quality information in the height of the peak, which is proportional to the

* Corresponding author. Tel.: +49 421 218 58114

E-mail address: westermeyer@bias.de

intensity of the probe beam reflected from that depth.

Ideally the probe beam is reflected at the keyhole bottom, giving a correct value for the weld depth. However, as the keyhole fluctuates so does the OCT measurement. In some cases the probe beam can be reflected at the keyhole wall, giving a too low measurement for the keyhole depth while in others it may be reflected multiple times, producing a too high measurement. This makes statistical filtering necessary to determine a keyhole depth from the OCT-data, taking a certain window of datapoints into account. The most commonly employed filtering method is a percentile filter, where the weld depth is selected as a certain percentile value of the datapoints inside the window (Authier et al. 2016). As this percentile is process specific, it has to be calibrated by metallographic cross sections for every material and welding parameter combination. Applying noise reduction methods prior to percentile filtering shows increased robustness for different welding conditions (Boley et al. 2019). Another method for filtering OCT data that was proven to be process and material independent is histogram filtering as shown by (Mittelstädt et al., 2019). Here, a histogram of OCT-datapoints over the depth is created and the last local peak (LLP) associated with the keyhole bottom is representative of the weld depth. By additionally scaling the counts of the histogram by the quality of each datapoint (Pordzik et al., 2023) were able to increase the measurement's reliability.

Generally, the amount of datapoints needed to obtain a reliable weld depth measurement is larger for histogram-based filters compared to percentile filtering. As the inclusion of more past datapoints also produces a slower reaction to fast fluctuations in the weld depth, investigations on whether these filters are suitable for a closed loop control system are necessary. This study first investigates how fast the weld depth changes during welds with constant parameters and secondly how fast the different filters react to sudden changes in the weld depth. Examinations on the former were made by measuring the weld depth over time in different materials (steel, aluminum and copper) and under different welding speeds in longitudinal cross sections. Tests on the filters themselves focus on the effects of different window sizes using simulated OCT-data for a controlled test environment.

Materials and methods

1.1. Laser welding setup

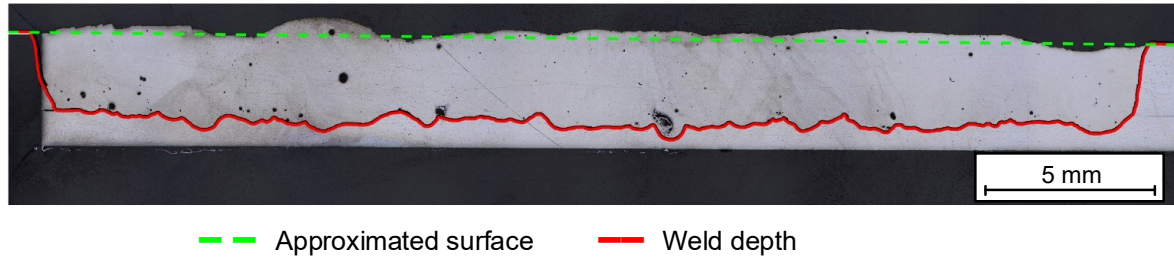
To measure the weld depth fluctuations for different materials, 38 mm long overlap weld seams through upper sheets with a thickness of 2 mm into lower sheets of 1 mm were made in Steel (DC-01), Aluminum (EN AW-1050), and Copper (CU-ETP). A TruDisk 12002 disk laser was utilized, which was guided through a fiber with a 200 μm core diameter and focused through a Precitec YW52 optic to a focal spot size of 200 μm . The weld seams in steel and aluminum were made with a welding speed of 4 m/min and 8 m/min. In copper a minimal welding speed of 6 m/min was needed to create welds with a sufficient quality, therefore the welds in copper were made with welding speeds of 6 m/min and 8 m/min. Argon was used as a shielding gas. For all combinations of materials and welding speed a critical laser power (P_{crit}) was experimentally determined for which a maximal welding depth could be achieved without producing weld through defects. The critical laser powers can be seen in Table 1. Longitudinal cross sections of three seams for each of the six parameter combinations were made for further evaluation.

Table 1. Critical laser powers used for the welding

Material	P_{crit} at 4m/min	P_{crit} at 6 m/min	P_{crit} at 8 m/min
DC-01	2400 W	-	3800 W
EN AW-1050	2500 W	-	3400 W
CU-ETP	-	6500 W	10250 W

1.2. Evaluation of longitudinal cross sections

The weld depth was extracted from the longitudinal cross section by manually marking the lower edge of the seams, which could then be automatically segmented by a MATLAB script. Additionally the surface of the upper sheet at the left and right edges was approximated by a second order polynomial to eliminate the influence of an angle in the image or a warping in the sheets. An exemplary longitudinal cross section of a weld seam in aluminum with marked surface and weld depth can be seen in Fig. 1. Knowing the welding speed, the length of the cross section was converted to a time vector, giving the actual weld depth over time. Sections with increasing weld depth were identified by zero crossings in the derivative of

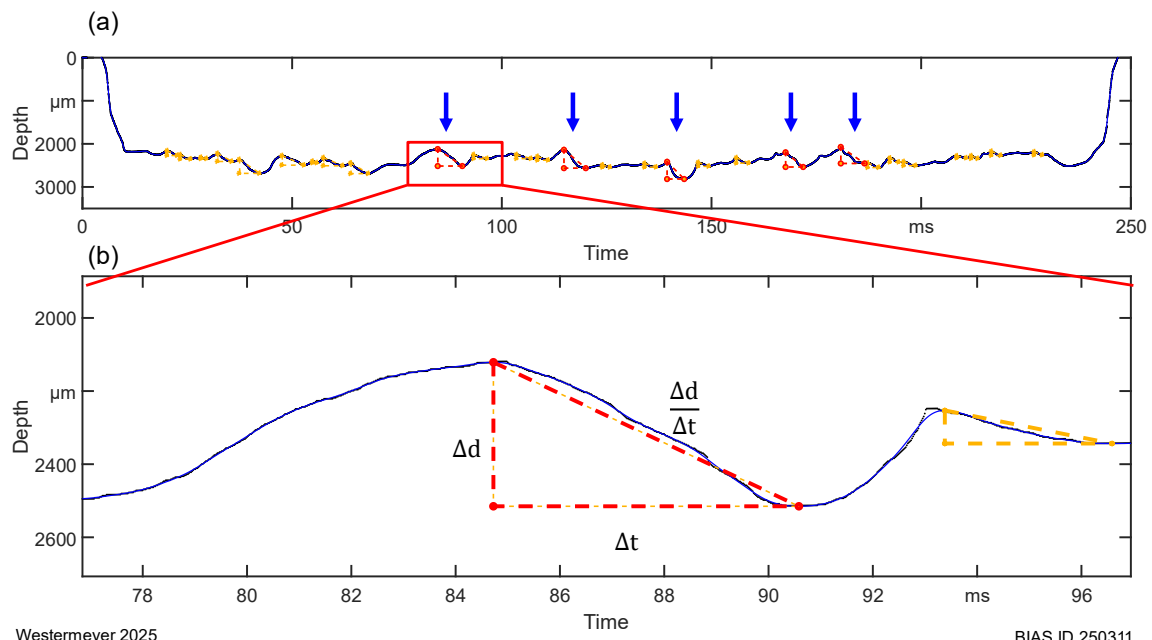


Westermeyer 2025

BIAS ID 250320

Fig. 1. Longitudinal cross section of a weld seam in aluminum (EN AW 1050), with the approximated surface and weld depth marked in green and red respectively.

the weld depth. Here a zero crossing from negative to positive indicates the start of a section with increasing weld depth and the next crossing from positive to negative its end. One exemplary extracted weld depth, with marked sections can be seen in Fig. 2. (a). In this manner all sections with an increasing weld depth were marked and their absolute depth increase (Δd) and duration in time (Δt) measured as shown in Fig. 2 (b). From these an average change rate ($\Delta d/\Delta t$) was calculated for each section. The five sections with the largest change rates from each cross section were selected, placing the emphasis on the major sections with the highest risk of producing weld through defects.



Westermeyer 2025

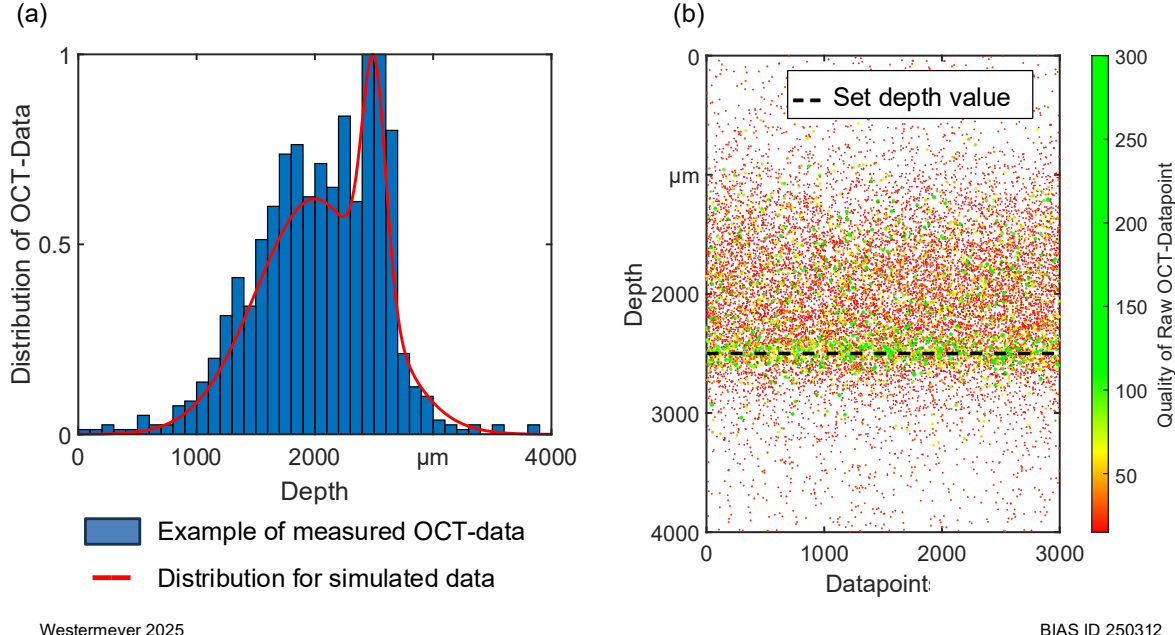
BIAS ID 250311

Fig. 2. (a) Extracted weld depth of one longitudinal cross section. Sections with increasing weld depth marked in yellow, five sections with the highest change rate marked in red; (b) Definitions of the absolute depth increase (Δd), duration in time (Δt) and change rate ($\Delta d/\Delta t$) for sections with increasing weld depth.

1.3. Simulation of OCT-data

For the filtering of OCT-data to be tested in a more controllable environment compared to real world data, which follows the fluctuating depth of the keyhole, test sets of OCT-data were simulated. The data is generated to resemble real world OCT-data of which a histogram can be seen in Fig. 3. (a). The histogram was approximated using the sum of two gaussian distributions, one broader acting as the OCT-signal originating from the keyhole walls and one sharper distribution as signal originating from the bottom of the keyhole. This distribution is used as the basis for simulating the OCT-data where the peak of the sharper gaussian is treated as the keyhole depth and thus the weld depth. To change the weld depth of the simulated OCT-data, the entire distribution is simply shifted to a different depth. In this manner, simulated OCT-data with a perfectly

constant depth or an arbitrary depth profile can be generated. In analogy to the data output by a Precitec IDM OCT-system six datapoints are generated at each point in time, resembling the first six peaks in the depth spectrum. Each one of these datapoints is comprised of a depth and a quality value. Four of the depth values were generated according to the distribution such that datapoints are more likely to be placed at a depth proportional to the distribution's height. To add a small amount of randomness to the depth values a randomly chosen value from -300 to 200 μm was added to every datapoint. In addition to the four depth values two noise values were added at each point in time which could take values 0 to 10000 μm . The quality value assigned to each datapoint also follows the distribution so that datapoints with a depth close to the keyhole bottom gain higher quality value, as would be the case in real OCT-data. In total ten sets of OCT-data were simulated, each containing 3000 timesteps. An exemplary dataset with a constant depth of 2500 μm can be seen in Fig. 3. (b).



Westermeyer 2025

BIAS ID 250312

Fig. 3. (a) Histogram of a real OCT-dataset with the distribution used as reference for the simulated OCT-data; (b) Example of simulated OCT-data with a constant depth set to 2500 μm .

1.4. Effects of window size on filter performance

Two main tests were conducted applying common filters to the simulated data. First the accuracy of the filter depending on the window size was tested on OCT-data with a constant depth. Here the absolute difference between the set depth value and the result of the filter was calculated at each point in time as seen in Fig. 4 (a). The steady state error was then calculated as the average absolute difference over all ten datasets. Secondly the reaction time of the filters to an increasing weld depth was measured. For this the weld depth was set to a constantly increasing value in the second half of the dataset. Different slopes of 0.5 μm , 1 μm , 2 μm , and 4 μm increase in weld depth each timestep were used to investigate effects of a more drastic increase in weld depth. The filters' reaction time was arbitrarily defined as the number of timesteps it took for the filtered weld depth to increase by 100 μm after the beginning of the downward slope as shown in Fig. 4 (b). The tests were done without an explicit timescale so that the results can be interpreted with different OCT measurement frequencies.

The effects of the window size (window of datapoints used for filtering) were tested with the simulated OCT-data. Overall window sizes from 1000 to 25 datapoints were used. The filters used were first a percentile filter, with its percentile value set to minimize the deviation from a constant depth of 2500 μm , a standard histogram filter, and a histogram filter with additional scaling based on the quality of the datapoint, henceforth named the quality filter.

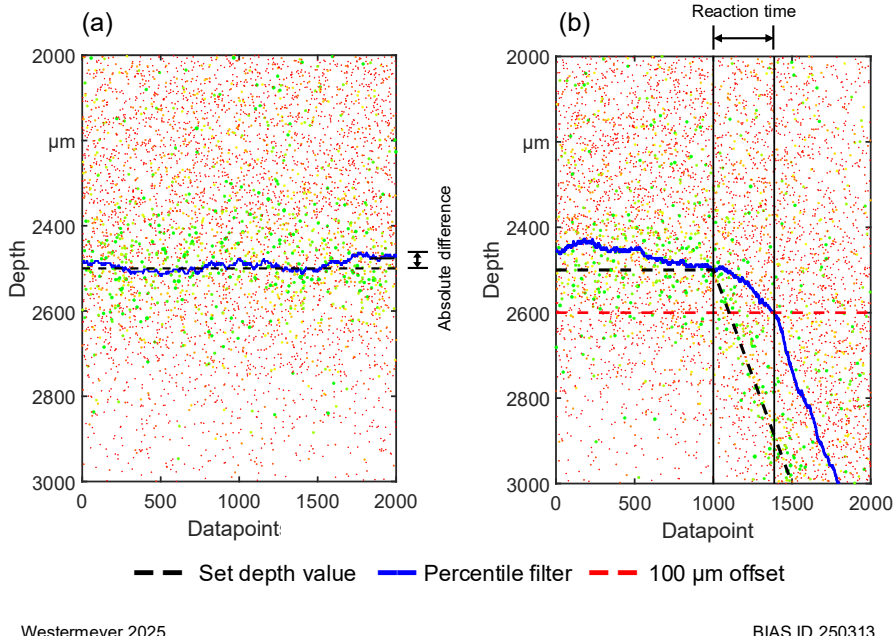


Fig. 4. Filter tests conducted on the simulated OCT-data with percentile filter as an example. (a) steady state error; (b) reaction time.

2. Results

2.1. Weld depth fluctuations

In Fig. 5. the absolute depth changes (Δd) of extracted sections with increasing weld depth are shown over their duration in time (Δt). Weld seams made in steel show the least weld depth fluctuations with the largest fluctuation not increasing more than 500 μm in 12 ms, independent from the welding speed. Seams in copper showed greater changes in weld depth, which also took place over longer durations with the largest increasing by more than 800 μm in 10 to 15 ms. A slight dependence on the weld speed can be seen in copper where seams welded with 8 m/min show a higher change rate compared to those welded at 6 m/min. Aluminum welds displayed the strongest fluctuations where in a few cases the weld depth increased by more than 700 μm less than 6 ms. In all graphs a black line indicates the highest change rate found in that material further demonstrating the three times higher change rates found in aluminum welds compared to those in steel, with copper being the intermediate.

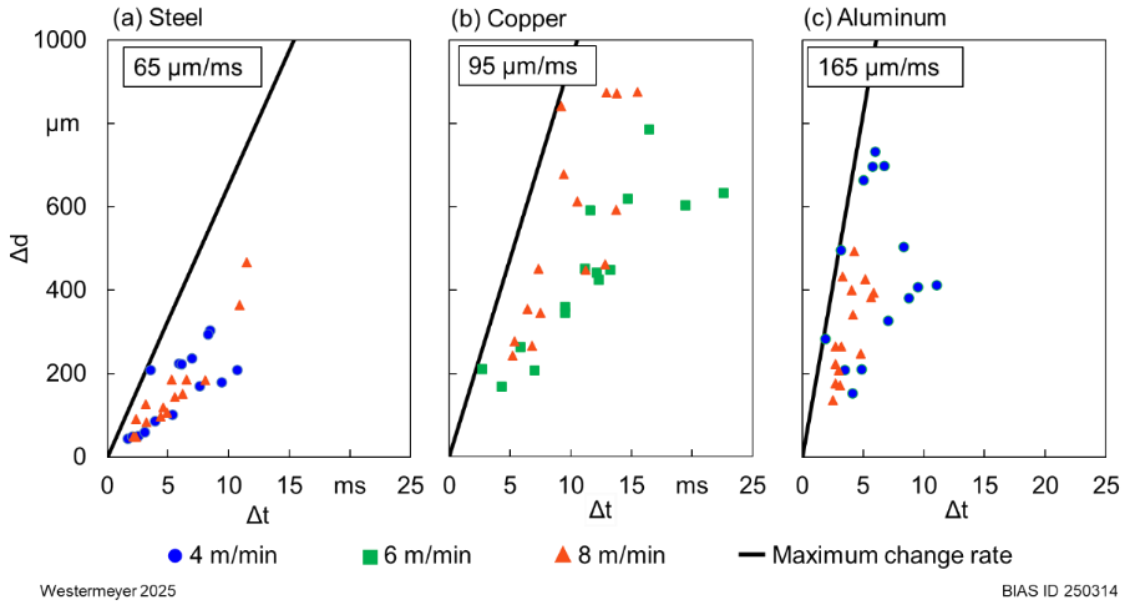


Fig. 5. Absolute depth changes (Δd) over duration in time (Δt) of sections with increasing weld depth extracted from longitudinal cross sections of weld seams in (a) Steel, (b) Copper and (c) Aluminum. A black line indicates the highest change rate for each material.

2.2. Steady state error

Fig. 6 shows the results for the first test on the simulated OCT-data, which examined the steady state error in dependence on the number of data points in the filter window. Here the percentile and quality filters performed significantly better than the histogram filter. This also demonstrates the advantage gained by the quality filter through the inclusion of the OCT-Data's quality values in filtering. Although the percentile value in the percentile filter was set to predict the constant set depth of 2500 μm with the most accuracy, the filter's output always varies slightly around this value. Thus the percentile filters' steady state accuracy is outperformed by the quality filter, whose accuracy is almost perfect, especially for windows sizes greater than 500. However the quality filter's accuracy is slightly increased compared to a real world scenario due to the set depth being a round value of 2500 μm , which coincides perfectly with the center of one of the histogram bins used

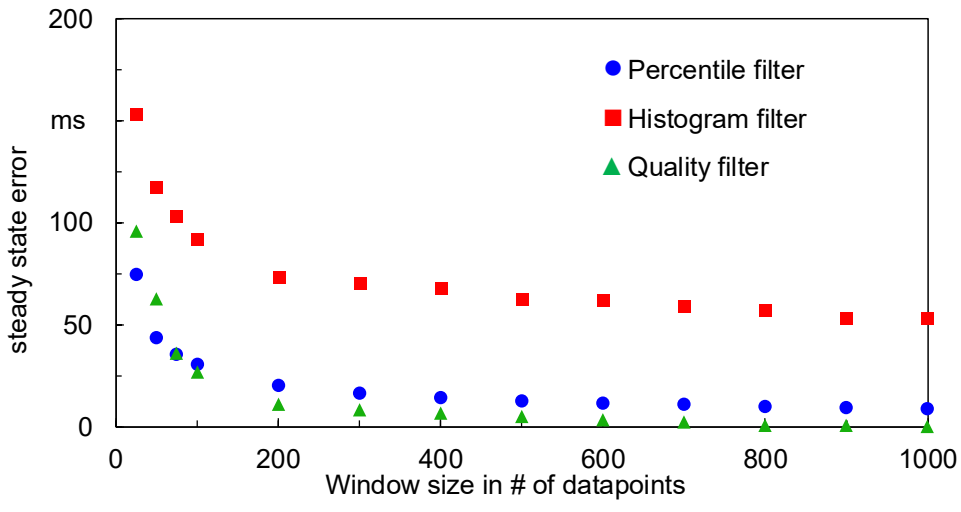


Fig. 6. Steady state error for the three different filter methods used as a function of the number of datapoints in the window used for filtering.

in the filter. Whenever a peak in the histogram bin corresponding to 2500 μm is detected by the quality filter, the absolute difference between set depth and the filtered depth becomes zero. While the percentile filter would be unaffected by an offset in the set depth of less than the size of one histogram bin (here 100 μm) this would produce an error in the quality filter equal to that offset. Furthermore the effects of a reduced window size are similar for all three filters. From a window size of 1000 to 200 datapoints used by the filters only a small increase in the steady state error can be seen, whereas below 200 datapoints a drastic increase takes place.

2.3. Reaction time

The reaction of the quality filter compared to the percentile filter to a slope of 1 μm per timestep is shown in Fig. 7, where a window size of 500 datapoints is used for both filters. Since the way the weld depth is determined in the histogram-based filters is fundamentally different to the percentile filter the mechanisms of how the filters react to the beginning of a downward slope are also different. When the filter window shifts over the beginning of a downward slope there are gradually more points with a higher depth added to the window, while points with an, on average, lower depth leave the window. This gradually shifts the entirety of all datapoints to greater weld depth, which also shifts the result of the percentile in the same direction. For the histogram-based filters this gradual shift causes an increase of counts in the histogram bins corresponding higher weld depths. However as these filters use the last local peak to determine the weld depth, an increase is only detected when a new higher peak at a higher weld depth is created. Thus the filtered weld depth can stay on one level long after the beginning of a downward slope. Additionally when two of the histogram bins have similar counts the randomness in the next datapoints may decide which becomes the peak, which can be seen as the filtered weld depth jumping up and down several times.

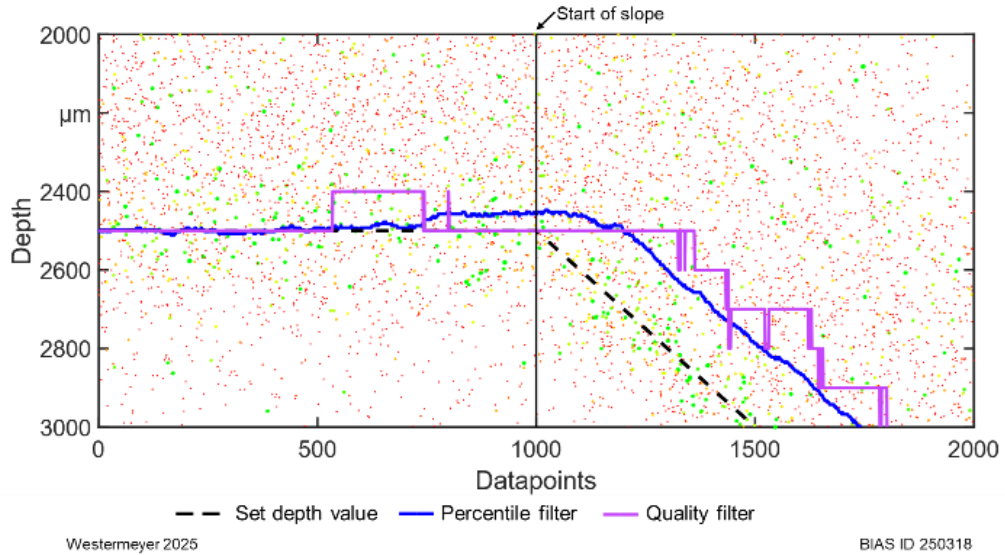


Fig. 7. Comparison of the reaction of the percentile and quality filters with a window size of 500 to a downward slope of 1 μm per timestep.

In testing the reaction time to an increasing depth in the simulated OCT-data the expected slower reaction with increasing window size was demonstrated. With a more gradually increasing weld depth as depicted in Fig. 8. (a), (b) large filter window sizes lead to a heavily delayed detection, especially for the histogram and quality filter. Differences between the filters become smaller as the window size decreases. At window sizes below 200 all filters reach the 100 μm detection threshold faster than the slope. These early detections are caused by the lower filter stability with decreasing window size and can be interpreted as false positives. Fig. 8. (c) and (d) show how filters react faster to a steep or very steep increase in weld depth, with the difference between the filters also becoming smaller. In the case of the percentile filter false positives are reduced with steeper slopes, while the histogram and quality filter show false positives for all tested slopes.

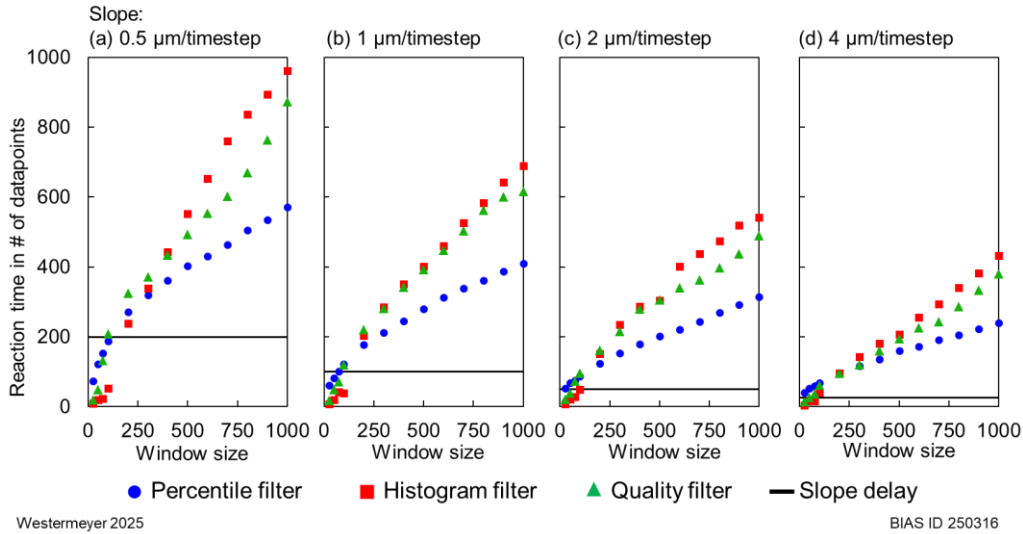


Fig. 8 Number of datapoints that it takes the filters to reach a 100 μm offset after the start of an increasing weld depth with different slopes of (a) 0.5 μm , (b) 1 μm , (c) 2 μm and (d) 4 μm depth increase each timestep. A black line indicates the number of datapoints that the slope itself takes to reach the detection threshold.

3. Discussion

When measuring an increasing weld depth with a certain change rate, higher measurement frequencies not only allow for more datapoints in the same amount of time, but also the apparent slope of the increasing depth becomes shallower. This is illustrated in Fig. 9 for the case of the highest change rate of 165 $\mu\text{m}/\text{ms}$ found in aluminum welds. Two measurement frequencies that are commonly found in today's OCT-systems (70 and 250 kHz) are highlighted there. Given a frequency of 70 kHz, the depth is only measured 44 times over the time it takes for the weld depth to increase by 100 μm with an apparent slope of 2.3 μm each timestep. At this low number of datapoints all filters exhibit a high steady state error, while the histogram and quality filter are prone to producing false positives. Thus an accurate detection of the fastest weld depth fluctuations may be inherently difficult. In contrast an increased OCT frequency of 250 kHz provides 156 depth measurements with an apparent slope of 0.6 μm per timestep. In this case using a more stable window size of around 200 can provide a reduced steady state error and a small detection delay is achieved with both quality and percentile filters. Further increases in the measurement frequency would make detection of weld depth fluctuations more reliable.

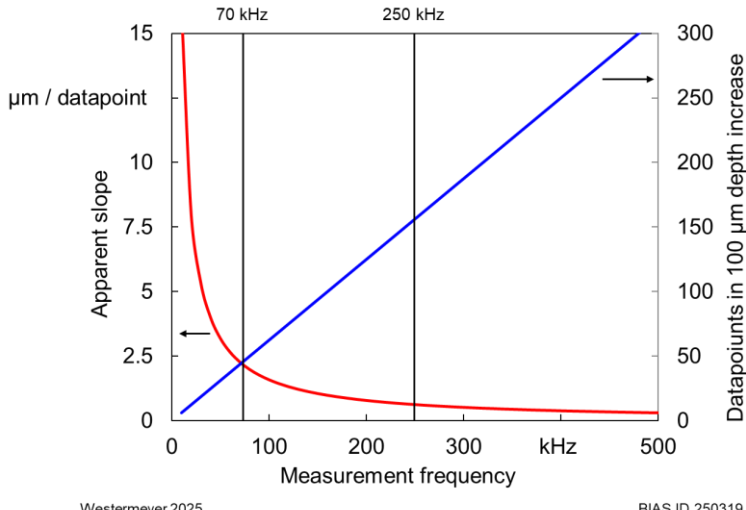


Fig. 9. Datapoints in 100 μm depth increase and apparent slope for different measurement frequencies for the case of an increasing weld depth with the highest change rate of 165 $\mu\text{m}/\text{ms}$ measured in an Aluminum weld seam.

4. Conclusions

In the first part of this study, investigations on severity of the weld depth fluctuations during laser welding were conducted. The welds made in steel showed the smallest weld depth fluctuation and the most severe were found in aluminum, with copper being the intermediate.

Secondly, tests regarding the effects of different amounts of datapoints used in filtering using common methods for filtering OCT-data were conducted on simulated OCT-data. Results showed how the reaction time of filters to a sudden change in weld depth can be reduced by using smaller window sizes. However filter accuracy strongly decreases when using window sizes of less than 200 datapoints, which can also lead to false positives when trying to detect increases in weld depth.

Using an OCT-system with a higher measurement frequency can alleviate these problems by providing more datapoints in the same amount of time and thus allowing to use more stable, larger window sizes in filtering.

Acknowledgements

The IGF-Project with the IGF-No.: 01IF23198N / DVS-No.: 06.3701 of the “Forschungsvereinigung Schweißen und verwandte Verfahren e. V.” of the German Welding Society (DVS), Aachener Str. 172, 40223 Düsseldorf was funded by the Federal Ministry for Economic Affairs and Energy (BMWE) via the German Aerospace Center (DLR) in accordance with the policy to support the Industrial Collective Research (IGF) on the basis of a decision by the German Bundestag.

Furthermore, the authors gratefully acknowledge the collaboration with the members of the project affiliated committee regarding the support of knowledge, material and equipment over the course of the research.

References

- Authier, N., Baptiste, A., Bruyere, V., Namy, P., Touvrey, C., 2016. Implementation of an interferometric sensor for measuring the depth of a capillary laser welding. In : International Congress on Applications of Lasers & Electro-Optics. ICALEO® 2016: 35th International Congress on Applications of Lasers & Electro-Optics. San Diego, California, USA, October 16–20, 2016: Laser Institute of America, p. 904.
- Bautze, T., Kogel - Hollacher, M., 2014. Keyhole Depth is just a Distance. *Laser Technik Journal* 11 (4), pp. 39 – 43.
- Boley, M., Fetzer, F., Weber, R., Graf, T., 2019. Statistical evaluation method to determine the laser welding depth by optical coherence tomography. *Optics and Lasers in Engineering* 119 (15), pp. 56–64.
- Fercher, A. F., Drexler, W., Hitzenberger, C. K., Lasser, T., 2003. Optical coherence tomography - principles and applications. *Rep. Prog. Phys.* 66 (2), pp. 239–303.
- Konuk, A. R., Aarts, R., Veld, A. H. i., Sibillano, T., Rizzi, D., Ancona, A., 2011. Process Control of Stainless Steel Laser Welding using an Optical Spectroscopic Sensor. *Physics Procedia* 12, pp. 744–751.
- Kos, M., Arko, E., Kosler, H., Jezeršek, M., 2021. Penetration-depth control in a remote laser-welding system based on an optical triangulation loop. *Optics and Lasers in Engineering* 139, p. 106464.
- Mittelstädt, C., Mattulat, T., Seefeld, T., Kogel-Hollacher, M., 2019. Novel approach for weld depth determination using optical coherence tomography measurement in laser deep penetration welding of aluminum and steel. *Journal of Laser Applications* 31 (2), p. 354.
- Pordzik, R., Ahlers, T., Mattulat, T., 2023. Enhancement of weld depth analysis in laser welding by extension of the oct data scope.